Arch. Mech., **65**, 1, pp. 55–66, Warszawa 2013

Brief Note

Nonlinear deformation of a tapered elastica cantilever due to a tip load

C. Y. WANG

Department of Mathematics
Michigan State University
East Lansing, MI 48824, U.S.A.
e-mail: cywang@mth.msu.edu

The nonlinear large deformation of a tip loaded tapered cantilever is studied. Different cross sectional shapes, deformation directions, tapers, base inclinations and end loads are considered. Explicit stability characteristic equations are given. Asymptotic analysis gives good approximations for large tip loads ($p > 20$). Deformation properties of the tapered cantilever are discussed.

Key words: elastica, taper, cantilever, large deformations.

1. Introduction

The elastica models are very flexible thin rods which can sustain large deformations. The theory of elastica was formulated by Euler [1] and given in the seminal work of Love [2] and Frisch-Fay [3]. There are basically two types of loads that deform the elastica, namely body forces such as self weight and point forces (and moments) which are usually applied at the ends. The governing equations, solutions and results are quite different for these two types.

Most literature in the elastica theory considered uniform cross sections. There are few reports for the non-uniform tapered elastica. In a recent paper, Wang [4] studied the large deformations of the tapered elastica under self weight. The present Note considers the other fundamental type, i.e., the tapered elastica deformed by a tip load. This situation occurs in load bearing robotic arms and other flexible mechanisms where the self weight of the elastica can be neglected in comparison to the effects of the tip load.

There are several sources which considered the tapered elastica deformed by a tip load. Raju and Rao [5] solved the elastica column with linearly varying similar cross sections under an axial load. Lee *et al.* [6] considered the constant thickness elastica cantilever with linearly tapered sides under a transverse load. Of interest is the work of Holland *et al.* [7] who studied the tapered, constant thickness column with an inclined tip load. Their experiments confirm numerical results superbly. These sources studied smaller post-buckling deformations. The present work considers large deformations of four different tapers, using both numerical and asymptotical methods.

2. Formulation and stability

Figure 1 shows an elastica cantilever with a tip load. The angle between the load P and the base inclination is γ. When $\gamma = 0$ the undeformed cantilever is vertical, and when $\gamma = \pi/2$ it is a horizontal cantilever. Let s' be the arc length from the base and θ be the local inclination after deformation. A local moment balance on an elemental segment gives

$$\frac{d}{ds'}\left(EI\frac{d\theta}{ds'}\right) + P'\sin\theta = 0. \tag{2.1}$$

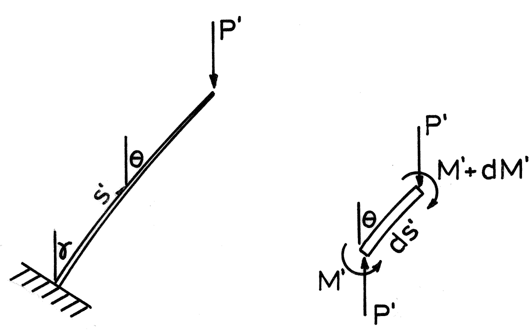

FIG. 1. Tip load P'on an inclined cantilever.

Normalize all lengths by the elastica length L and drop primes. Let EI_0 be the flexural rigidity at the larger fixed (base) end, and

$$EI = EI_0\, l(s). \tag{2.2}$$

Equation (2.1) becomes

$$\frac{d}{ds}\left(l(s)\frac{d\theta}{ds}\right) + p\sin\theta = 0, \tag{2.3}$$

where $p = P'L^2/EI_0$ is the normalized load. The boundary conditions are

$$\theta(0) = \gamma, \tag{2.4}$$

$$\frac{d\theta}{ds}(1) = 0. \tag{2.5}$$

For linearly tapered cantilevers, the rigidity function $l(s)$ can be expressed as

$$l(s) = (1 - cs)^m, \tag{2.6}$$

where $0 \leq c \leq 1$ and $m \geq 0$ are constants. The cantilever is uniform if $c = 0$ or $m = 0$. If the cross section is doubly tapered (as a cone) then $m = 4$. If the thickness is constant but the width tapers and the cantilever bends in the thickness direction, then $m = 1$. If it bends in the width direction then $m = 3$. If the cantilever is composite with surface material separated by a tapered low density filling, then $m = 2$. Note that [5] considered only $m = 4$ and [6, 7] only $m = 1$.

When the load is an axial compression, $\gamma = 0$. The cantilever would remain straight until a critical load is reached. Linearization of Eq. (2.3) for small θ gives the equation

$$\frac{d}{ds}\left((1 - cs)^m \frac{d\theta}{ds}\right) + p\theta = 0. \tag{2.7}$$

With the boundary conditions

$$\theta(0) = 0, \qquad \frac{d\theta}{ds}(1) = 0. \tag{2.8}$$

This stability problem was solved by DINNIK [8] for doubly-tapered columns, which are equivalent to fixed-free cantilevers. Here we shall give some explicit stability solutions. Let

$$z = 1 - cs, \qquad \mu = \sqrt{p}/c. \tag{2.9}$$

Equation (2.3) becomes

$$\frac{d}{dz}\left(z^m \frac{d\theta}{dz}\right) + \mu^2\theta = 0. \tag{2.10}$$

For $m = 1$ the independent solutions are in terms of the Bessel functions $J_0(2\mu\sqrt{z})$ and $Y_0(2\mu\sqrt{z})$ [9]. Applying the boundary conditions Eq. (2.8) at $z = 1$ and $z = 1 - c$ gives the characteristic equation ($c \neq 1$)

$$Y_0(2\mu)J_1(2\mu\sqrt{1-c}) - J_0(2\mu)Y_1(2\mu\sqrt{1-c}) = 0 \tag{2.11}$$

from which the buckling load p can be obtained easily by bisection.

For $m = 2$ the independent solutions are

$$z^{-1/2}\sin(\sqrt{\mu^2 - 1/4}\ln z) \qquad \text{and} \qquad z^{-1/2}\cos(\sqrt{\mu^2 - 1/4}\ln z).$$

The boundary conditions give

$$\tan[\sqrt{\mu^2 - 1/4}\ln(1-c)] - 2\sqrt{\mu^2 - 1/4} = 0. \tag{2.12}$$

For $m = 3$ the independent solutions are $z^{-1}J_2(2\mu/\sqrt{z})$ and $z^{-1}Y_2(2\mu/\sqrt{z})$. The characteristic equation is

$$J_2(2\mu)Y_1(2\mu/\sqrt{1-c}) - Y_2(2\mu)J_1(2\mu/\sqrt{1-c}) = 0. \tag{2.13}$$

For $m = 4$ let $\varsigma = \mu/z$. After some work, Eq. (2.10) becomes

$$\frac{d^2\theta}{d\varsigma^2} - \frac{2}{\varsigma}\frac{d\theta}{d\varsigma} + \theta = 0. \tag{2.14}$$

The independent solutions are $\cos\varsigma + \varsigma\sin\varsigma$ and $\sin\varsigma - \varsigma\cos\varsigma$. The characteristic equation is then

$$(\cos\mu + \mu\sin\mu)\sin[\mu/(1-c)] - (\sin\mu - \mu\cos\mu)\cos[\mu/(1-c)] = 0. \tag{2.15}$$

Table 1 shows a comparison of our results with Dinnik's values [8]. Dinnik used the ratio of the end moment of inertia $i : I$ related to our taper factor c by $c = 1 - (i : I)^{1/m}$. Also, the buckling load of Dinnik's pinned-pinned symmetric taper is four times the cantilever buckling load. We see the values are very close, except for $m = 4$ and $i : I = 0.1$, which we suspect to be a typo in Dinnik's entry.

Table 1. Comparisons of critical loads with those from Dinnik [8].

	$i : I$	c	$4p$ (Dinnik)	$4p$ (present)
m=1	0.2	0.8	7.01	7.008
	0.8	0.2	9.27	9.262
m=2	0.1	0.6838	5.40	5.399
	0.8	0.1056	9.24	9.243
m=3	0.2	0.4152	6.14	6.136
	0.8	0.1717	9.23	9.236
m=4	0.1	0.4377	4.31	4.812
	0.8	0.0543	9.23	9.232

The buckling loads using our formulas are given in Table 2. Of course, when $c = 0$ or $m = 0$ the cantilever is uniform and the buckling load is $\pi^2/4 = 2.4674$. For $c = 1$ the cantilever diminishes into a sharp point, and is unlikely to support any tip load.

Table 2. The critical load p_{cr} for various cross sections m and tapers c.

$m\backslash c$	0.1	0.2	0.3	0.4	0.5	0.6	0.7	0.8	0.9
1	2.393	2.316	2.235	2.151	2.062	1.968	1.865	1.752	1.621
2	2.319	2.167	2.012	1.851	1.683	1.507	1.318	1.109	0.862
3	2.246	2.023	1.798	1.569	1.336	1.099	0.853	0.597	0.321
4	2.175	1.883	1.595	1.309	1.029	0.757	0.498	0.264	0.0804

3. Asymptotic analysis

For large p the elastica cantilever becomes highly deformed and an asymptotic solution is possible. We shall use the boundary layer method. Let

$$\varepsilon = \frac{1}{\sqrt{p}} \ll 1. \tag{3.1}$$

Equation(2.3) is singular

$$\varepsilon^2 \frac{d}{ds}\left((1-cs)^m \frac{d\theta}{ds}\right) + \sin\theta = 0. \tag{3.2}$$

The interior solution satisfying $\sin\theta = 0$ is $\theta = n\pi$. We can take $n = 1$ without loss of generality since γ can vary. Inside the boundary layer near the base, let

$$s = \varepsilon t \tag{3.3}$$

and expand

$$\theta = \theta_0(t) + \varepsilon mc\theta_1(t) + O(\varepsilon^2). \tag{3.4}$$

Equating like orders of ε, Eq. (3.2) yields the first two orders

$$\frac{d^2\theta_0}{dt^2} + \sin\theta_0 = 0, \tag{3.5}$$

$$\frac{d^2\theta_1}{dt^2} + (\cos\theta_0)\,\theta_1 = \frac{d}{dt}\left(t\frac{d\theta_0}{dt}\right). \tag{3.6}$$

The boundary conditions Eqs. (2.4) and (2.5) are

$$\theta_0(0) = \gamma, \qquad \theta_0(\infty) = \pi, \tag{3.7}$$

$$\theta_1(0) = 0, \qquad \theta_1(\infty) = 0. \tag{3.8}$$

Multiply Eq. (3.5) by $d\theta_0/dt$ and integrate to obtain

$$\frac{d\theta_0}{dt} = 2\cos\left(\frac{\theta_0}{2}\right). \tag{3.9}$$

With the boundary conditions Eq. (3.7) the solution is found to be

$$\theta_0 = \pi - 4\tan^{-1}[ge^{-t}], \qquad g = 1/\tan[(\gamma+\pi)/4]. \tag{3.10}$$

Eq. (3.10) is substituted into Eq. (3.6). We are fortunate to obtain an analytic solution as follows. Guided by Eq. (3.10), let

$$u = ge^{-t}. \tag{3.11}$$

After some work, Eq. (3.6) becomes

$$u(1+u^2)^2\frac{d}{du}\left(u\frac{d\theta_1}{du}\right) - (u^4-6u^2+1)\theta_1 = 4u[(1+u^2)+\ln\left(\frac{u}{g}\right)(1-u^2)] = 0. \tag{3.12}$$

The homogeneous solutions are $u/(1+u^2)$, $(u^4+4u^2\ln u-1)/[2u(1+u^2)]$ and the particular solution is $u\{u^2-1+2[(1+2\ln u)\ln(u/g)-(\ln u)^2]\}/[2(1+u^2)]$. Using the boundary conditions

$$\theta_1|_{u=0} = 0, \qquad \theta_1|_{u=g} = 0 \tag{3.13}$$

the solution is

$$\theta_1 = \frac{u\{u^2-g^2+2[(1+2\ln u)\ln(u/g)-(\ln u)^2+(\ln g)^2]\}}{2(1+u^2)}. \tag{3.14}$$

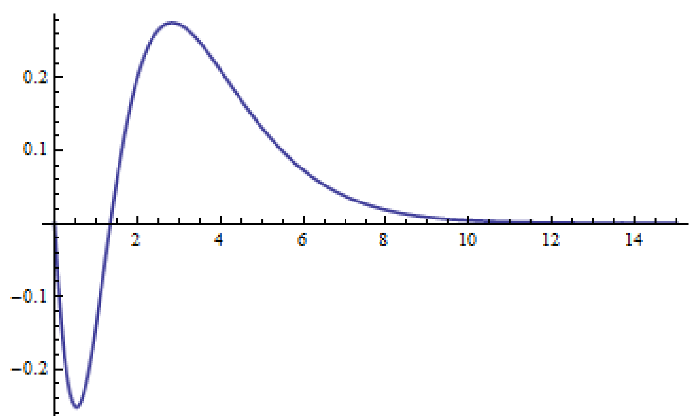

Fig. 2. First order boundary layer function $\theta_1(t)$ versus t ($\gamma = 0$).

Figure 2 shows a typical profile for $\theta_1(t)$. From Eq. (3.14) we find the simple result

$$\frac{d\theta_1}{dt}(0) = -g = \frac{-1}{\tan((\gamma+\pi)/4)}. \tag{3.15}$$

The normalized moment at the base is then

$$
\begin{aligned}
M_0 &= \frac{d\theta}{ds}(0) \\
&= \frac{1}{\varepsilon}\left[\frac{d\theta_0}{dt}(0) + \varepsilon mc\frac{d\theta_1}{dt}(0) + O(\varepsilon^2)\right] \\
&= 2\cos\left(\frac{\gamma}{2}\right)\sqrt{p} - \frac{mc}{\tan((\gamma+\pi)/4)} + O(p^{-1/2}).
\end{aligned}
\tag{3.16}
$$

Note that the effect of taper is in the $O(1)$ term of Eq. (3.16).

4. Numerical results

For general post-buckling, analytic solution does not exist and numerical integration is necessary. For given c, m, $p > p_{cr}$ Eq. (2.3) is integrated as an initial value problem using $\theta(0) = \gamma$ and a guessed normalized base moment $M_0 = \theta'(0)$. At $s = 1$ we check whether $\theta'(1)$ is zero. If not, M_0 is adjusted.

We compare our results with the limited previous literature. RAJU and RAO [5] studied the $m = 4$, $\gamma = 0$ case, with small taper ($c < 0.34$) and light loads ($p < 3.2$) while Lee et al [6] have data only for the $m = 1$, $\gamma = \pi/2$, $c = 0.667$ and $p = 1.667$ case. The results of HOLLAND *et al.* [7] are presented as graphs, and cannot be accurately compared. Some authors also included the self weight of the cantilever, which complicates the effects and does not apply to the present study. Table 3 shows a comparison.

Table 3. Comparison with previous works.

m	γ	c	p	M_0
4	0	0.3333	1.5872	0.5581 (present) 0.5581 [5]
4	0	0.3333	1.9020	1.1728 (present) 1.1737 [5]
1	$\pi/2$	0.6667	1.6667	1.3882 (present) 1.3870 [6]

We see that our results agree with previous literature. In the following, we shall present more comprehensive results, especially for large deformations.

First take the originally vertical cantilever ($\gamma = 0$). Only this case, with a vertical compressive load, is susceptible to buckling. Tables 4–7 show the results.

Table 4. Base moment M_0 for $\gamma = 0$ and $m = 1$. Zero entries denote buckling load has not been reached. Values in parenthesis are obtained from Eq. (3.16).

$p \backslash c$	0.1	0.3	0.5	0.7	0.9
2	0	0	0	0.816	1.184
5	3.937	3.843	3.727	3.583	3.399
10	6.144	5.964	5.771	5.564	5.338
20	8.836 (8.84)	8.635 (8.64)	8.427 (8.64)	8.212 (8.64)	7.990 (8.64)
50	14.042 (14.04)	13.839 (13.84)	13.633 (13.64)	13.423 (13.44)	13.210 (13.24)
100	19.900 (19.90)	19.698 (19.70)	19.494 (19.50)	19.287 (19.30)	19.078 (19.10)

Table 5. Base moment M_0 for $\gamma = 0$ and $m = 2$. Zero entries denote buckling load has not been reached. Values in parenthesis are obtained from Eq. (3.16).

$p \backslash c$	0.1	0.3	0.5	0.7	0.9
2	0	0	1.144	1.342	1.255
5	3.895	3.692	3.440	3.145	2.821
10	6.059	5.708	5.348	4.986	4.628
20	8.739 (8.74)	8.350 (8.74)	7.966 (7.94)	7.588 (7.94)	7.217 (7.94)
50	13.943 (13.94)	13.547 (13.54)	13.156 (13.14)	12.769 (13.14)	12.387 (13.14)
100	19.800 (19.80)	19.403 (19.40)	19.010 (19.00)	18.619 (18.60)	18.232 (18.20)

Table 6. Base moment M_0 for $\gamma = 0$ and $m = 3$. Zero entries denote buckling load has not been reached. Values in parenthesis are obtained from Eq. (3.16).

$p \backslash c$	0.1	0.3	0.5	0.7	0.9
2	0	0.975	1.353	1.271	0.525
5	3.851	3.531	3.151	2.755	2.389
10	5.975	5.464	4.968	4.503	4.077
20	8.644 (8.64)	8.081 (8.04)	7.548 (7.44)	7.0458 (6.84)	6.572 (6.24)
50	13.845 (13.84)	13.266 (13.24)	12.708 (12.64)	12.171 (12.04)	11.653 (11.44)
100	19.702 (19.70)	19.117 (19.10)	18.547 (18.50)	17.992 (17.90)	17.451 (17.30)

Table 7. Base moment M_0 for $\gamma = 0$ and $m = 4$. Zero entries denote buckling load has not been reached. Values in parenthesis are obtained from Eq. (3.16).

$p \backslash c$	0.1	0.3	0.5	0.7	0.9
2	0	1.239	1.339	1.109	0.874
5	3.805	3.367	2.882	2.438	2.070
10	5.892	5.233	4.630	4.100	3.637
20	8.550 (8.54)	7.827 (7.74)	7.168 (6.94)	6.569 (6.14)	6.025 (5.34)
50	13.748 (13.74)	12.995 (12.94)	12.287 (12.14)	11.621 (11.34)	10.995 (10.54)
100	18.907 (19.60)	18.838 (18.80)	18.104 (18.00)	17.401 (17.20)	16.728 (16.40)

The numerical integration however, becomes very sensitive to the initial guess of M_0 for large p. At $p = 100$, eight or nine correct digits are needed for a satisfactory solution. But for large p our asymptotic solution becomes accurate and thus can be utilized.

If $\gamma \neq 0$, there is no buckling load. The abridged results are shown in Tables 8–11. Values in parenthesis are from the asymptotic formula Eq. (3.16).

Table 8. Base moment M_0 for $m = 1$. Values in parenthesis are obtained from Eq. (3.16).

	$\gamma = \pi/4$			$\gamma = \pi/2$			$\gamma = 3\pi/4$		
$p \backslash c$	0.1	0.5	0.9	0.1	0.5	0.9	0.1	0.5	0.9
1	0.881	0.897	0.915	0.941	0.901	0.941	0.565	0.551	0.531
2	1.896	1.873	1.804	1.668	1.616	1.537	0.944	0.911	0.867
5	3.881	3.695 (3.80)	3.456 (3.53)	3.033 (3.12)	2.906 (2.96)	2.754 (2.79)	1.655 (1.69)	1.592 (1.61)	1.518 (1.53)
10	5.739 (5.78)	5.484 (5.51)	5.202 (5.24)	4.412 (4.43)	4.253 (4.27)	4.080 (4.10)	2.393 (2.40)	2.316 (2.32)	2.233 (2.24)
20	8.193 (8.20)	7.921 (7.93)	7.637 (7.66)	6.281 (6.28)	6.113 (6.12)	5.939 (5.95)	3.402 (3.40)	3.322 (3.32)	3.239 (3.24)
50	13.00 (13.00)	12.73 (12.73)	12.45 (12.46)	9.959 (9.96)	9.791 (9.79)	9.620 (9.63)	5.392 (5.39)	5.312 (5.31)	5.230 (5.23)
100	18.41 (18.41)	18.14 (18.14)	17.87 (17.88)	14.10 (14.10)	13.93 (13.94)	13.76 (13.77)	7.634 (7.63)	7.554 (7.55)	7.472 (7.48)

Table 9. Base moment M_0 for $m = 2$. Values in parenthesis are obtained from Eq. (3.16).

	$\gamma = \pi/4$			$\gamma = \pi/2$			$\gamma = 3\pi/4$		
$p\backslash c$	0.1	0.5	0.9	0.1	0.5	0.9	0.1	0.5	0.9
1	0.885	0.914	0.892	0.938	0.904	0.825	0.562	0.532	0.482
2	1.893	1.817	1.595	1.657	1.544	1.370	0.937	0.870	0.780
5	3.840 (3.90)	3.469 (3.46)	3.047 (2.93)	3.004 (3.08)	2.757 (2.75)	2.492 (2.42)	1.640 (1.67)	1.518 (1.51)	1.389 (1.35)
10	5.680 (5.71)	5.197 (5.18)	4.723 (4.64)	4.375 (4.39)	4.073 (4.06)	3.780 (3.73)	2.374 (2.38)	2.229 (2.22)	2.088 (2.06)
20	8.128	7.613	7.119	6.241	5.921	5.616	3.383	3.229	3.083
50	12.93 (12.93)	12.41 (12.40)	11.90 (11.86)	9.917 (9.92)	9.593 (9.59)	9.278 (9.25)	5.372 (5.37)	5.217 (5.21)	5.065 (5.05)
100	18.34 (18.34)	17.82 (17.81)	17.30 (17.28)	14.06 (14.06)	13.73 (13.73)	13.41 (13.40)	7.614 (7.61)	7.457 (7.46)	7.304 (7.30)

Table 10. Base moment M_0 for $m = 3$. Values in parenthesis are obtained from Eq. (3.16).

	$\gamma = \pi/4$			$\gamma = \pi/2$			$\gamma = 3\pi/4$		
$p\backslash c$	0.1	0.5	0.9	0.1	0.5	0.9	0.1	0.5	0.9
1	0.888	0.922	0.790	0.935	0.875	0.735	0.559	0.511	0.432
2	1.889	1.733	1.392	1.645	1.466	1.227	0.929	0.827	0.706
5	3.799 (3.93)	3.255 (3.46)	2.732	2.976 (3.04)	2.618 (2.54)	2.285	1.626 (1.65)	1.449 (1.41)	1.287 (1.17)
10	5.621 (5.64)	4.938 (4.84)	4.339	4.338 (4.35)	3.909 (3.85)	3.533	2.357 (2.36)	2.149 (2.12)	1.967 (1.88)
20	8.064 (8.06)	7.331 (7.26)	6.679	6.201 (6.20)	5.746 (5.70)	5.338 (5.21)	3.364 (3.36)	3.144 (3.12)	2.948 (2.89)
50	12.87 (12.87)	12.11 (12.06)	11.40 (11.26)	9.877 (9.88)	9.406 (9.38)	8.968 (8.88)	5.353 (5.35)	5.126 (5.11)	4.915 (4.88)
100	18.28 (18.28)	17.51 (17.48)	16.78 (16.67)	14.02 (14.02)	13.54 (13.52)	13.09 (13.02)	7.614 (7.59)	7.457 (7.36)	7.304 (7.12)

Table 11. Base moment M_0 for $m = 4$. Values in parenthesis are obtained from Eq. (3.16).

	$\gamma = \pi/4$			$\gamma = \pi/2$			$\gamma = 3\pi/4$		
$p\backslash c$	0.1	0.5	0.9	0.1	0.5	0.9	0.1	0.5	0.9
1	0.892	0.911	0.698	0.932	0.839	0.661	0.556	0.488	0.392
2	1.883	1.632	1.240	1.634	1.386	1.115	0.922	0.785	0.648
5	3.757 (3.86)	3.060	2.486	2.947 (3.00)	2.491	2.185	1.612 (1.63)	1.387 (1.31)	1.203
10	5.564 (5.58)	4.705	4.022	4.301 (4.31)	3.762 (3.64)	3.326	2.339 (2.34)	2.077 (2.02)	1.865
20	8.001 (8.00)	7.073 (6.93)	6.297	6.162 (6.16)	5.563 (5.50)	5.094	3.345 (3.34)	3.065 (3.03)	2.828 (2.71)
50	12.80 (12.80)	11.83 (11.73)	10.96 (10.66)	9.837 (9.83)	9.228 (9.17)	8.684 (8.51)	5.334 (5.33)	5.044 (5.01)	4.778 (4.70)
100	18.21 (18.21)	17.21 (17.14)	16.29 (16.07)	13.98 (13.98)	13.36 (13.31)	12.78 (12.65)	7.575 (7.57)	7.275 (7.26)	6.997 (6.94)

Figure 3 shows some typical deformations due to tip load p.

FIG. 3. Effect of tip load on deformation ($m = 4$, $c = 0.5$, $\gamma = 0$).
From top: $p < 1.029$, 1.5, 2, 10, 50.

5. Discussion

This paper presents the complete characteristics of the large deformations of a tapered cantilever. Unlike uniform cantilevers, where exact solutions in terms of elliptic functions exist, tapered cantilevers have no analytic solutions.

In comparison to the heavy tapered cantilever described in [4], there are some similarities but also many differences. The governing equations, stability criteria, and asymptotic forms are all different. Even the geometry of the heavy elastica is governed by two exponents while the tip loaded elastica only one. Also, exact stability criteria exist only for the pointy heavy elastica, while the tip loaded elastica has exact stability solutions only for the blunt tip. The post-buckling results show similar trends, but the numerical values are different.

In this paper, all important cross sectional shapes, deformation axes, tapers, base inclinations and end loads are studied. Explicit stability characteristic equations are given. Our asymptotic analysis is especially useful, since it gives accurate solutions for large tip loads ($p > 20$), for which the numerical scheme becomes too sensitive due to the stiffness of the nonlinear governing equation.

Our results are given in the base moment M_0, which serves as an initial value for integrating the deformed profiles. The lateral reach of the cantilever is M_0/p.

For buckling of the vertical cantilever, the critical load p_{cr} decreases for increased taper c and increase cross section factor m. Remember however, the critical load is normalized with respect to the base rigidity EI_0 which differs for each cross section.

For post buckling, holding other parameters fixed, the base moment increases with increased tip load p. When the taper c is increased, the base moment decreases for large p, but the base moment first increases then decreases for low p. The base moment also decreases for increased m and increases base inclination γ.

Instead of graphs, our tables would be useful in the design of load carrying tapered cantilevers.

References

1. L. Euler, *De Curvis Elasticis*, 1744.
2. A.E.H. Love, *A Treatise on the Mathematical Theory of Elasticity*, Dover, New York, 1944.
3. R. Frisch-Fay, *Flexible Bars*, Butterworths, Wash. D.C. 1962.
4. C.Y. Wang, *Large post-buckling of heavy tapered elastica cantilevers and its asymptotic analysis*, Arch. Mech., **64**, 207–220, 2012.
5. P.C. Raju, G.V. Rao, *Post-buckling analysis of tapered cantilever columns*, Comp. Meth. Appl. Mech. Eng., **15**, 201–206, 1978.
6. B.K. Lee, J.F. Wilson, S.J. Oh, *Elastica of cantilevered beams with variable cross sections*, Int. J. Nonlinear Mech., **28**, 579–589, 1993.
7. D.B. Holland, L.N. Virgin, R.H. Plaut, *Large deflections and vibration of a tapered cantilever pulled at its tip by a cable*, J. Sound Vibr., **310**, 433–441, 2008.
8. A. Dinnik, *Design of columns of varying cross sections*, Trans. ASME, **54**, 105–109, 1932.
9. G.M. Murphy, *Ordinary Differential Equations and Their Solutions*, Van Nostrand, Princeton, New Jersey, 1960.

Received July 10, 2012; revised version August 14, 2012.